Journal of The Electrochemical Society, **161** (6) A856-A862 (2014)
0013-4651/2014/161(6)/A856/7/$31.00 © The Electrochemical Society

Evaluation of the Electrochemical Performance of a Lithium-Air Cell Utilizing Diethylene Glycol Diethyl Ether-Based Electrolyte

Sang-Min Han, Jae-Hong Kim, and Dong-Won Kim[*,z]

Department of Chemical Engineering, Hanyang University, Seungdong-Gu, Seoul 133-791, Korea

Diethylene glycol diethyl ether (DEGDEE) was evaluated as an electrolyte solvent for a non-aqueous lithium-air cell. An electrolyte solution of 1 M LiTFSI in DEGDEE showed a high ionic conductivity of 4.7 mS cm^{-1} at room temperature and considerably high oxidative stability. The full discharge and charge cycles of the lithium-air cells demonstrated that the DEGDEE-based electrolyte provided the unique ability to facilitate the reversible reduction and oxidation processes at the porous carbon electrode without a catalyst. The lithium-air cell employing the DEGDEE-based electrolyte exhibited fairly stable cycling behavior when the carbon loading was 0.5 mg cm^{-2} and the depth of discharge of the carbon electrode was limited to 1,000 mAh g^{-1}.
© 2014 The Electrochemical Society. [DOI: 10.1149/2.022406jes] All rights reserved.

Manuscript submitted January 17, 2014; revised manuscript received March 18, 2014. Published April 16, 2014.

Since the non-aqueous Li-air battery was reported in 1996, it has attracted much attention in recent years due to its high theoretical specific energy of 11,000 Wh kg^{-1}, which is close to that of conventional gas-powered engines.[1–3] The successful development of rechargeable Li-air batteries is critically dependent on the long-term stability of all battery components and the highly reversible formation and decomposition of Li_2O_2 as a desired discharge product.[4–8] Up to now, although much progress has been achieved, the reversibility of lithium-air batteries is still far from satisfactory because most organic electrolytes do not possess long-term chemical stability in the presence of the superoxide anion radical. Accordingly, many research works have focused on the development and characterization of a stable electrolyte solvent to support prolonged cycling in the lithium-air battery.[9–16] Recent studies have shown that linear ethers such as tetra(ethylene glycol) dimethyl ether (TEGDME) are more stable than organic carbonates against nucleophilic attack by superoxide produced upon discharge at the air cathode, and thus, are being considered as a preferred electrolyte solvent for Li-air batteries.[10,17–20] Although lithium-air batteries can be discharged and charged in a TEGDME-based organic electrolyte, the cycling causes irreversible chemical changes in the electrolyte, which results in poor reversibility upon cycling.

In this study, we employed diethylene glycol diethyl ether (DEGDEE) as an electrolyte solvent and evaluated its performance in a Li-air cell. DEGDEE was selected as the electrolyte solvent for the lithium-air cell, because it has a high ionic conductivity (4.7 mS cm^{-1} with 1 M LiTFSI), low viscosity and high oxidative stability exceeding 5.0 V vs. Li/Li^+, which are superior to those of TEGDME. The lithium-air cell assembled with the DEGDEE-based electrolyte and carbon electrode (without a catalyst) initially delivered a high discharge capacity of 6,219 mAh g^{-1} based on the weight of carbon in the air cathode. By constraining the carbon loading to 0.5 mg cm^{-2} and limiting the depth of discharge to 1,000 mAh g^{-1}, the cell operated effectively over many cycles without any decay of the capacity. To the best of our knowledge, this is the first time that the cycling performance of a lithium-air cell with a DEGDEE-based electrolyte has been demonstrated.

Experimental

Electrolyte preparation.— All solvents utilized in the electrolyte solution were anhydrous grade purity purchased from Sigma Aldrich and were used after drying using pre-dried 4A molecular sieve for several days. The electrolyte solution was prepared by dissolving 1.0 M lithium bis(trifluoromethane) sulfonyl imide (LiTFSI, Sigma Aldrich) in DEGDEE, TEGDME and diethylene glycol dibutyl ether (DEGDBE), respectively, inside a glove box filled with purified argon. LiTFSI was chosen as the salt because it has better stability against moisture and heat than $LiPF_6$. The water content in the electrolytes was determined to be less than 20 ppm by Karl Fischer titration using a Mettler-Toledo Coulometer.

Cell assembly.— The carbon-based air electrode was prepared by coating the N-methyl pyrrolidone (NMP)-based slurry containing Ketjen black EC300JD and a poly(vinylidiene fluoride) (PVDF) binder (8:2 by weight) on a gas diffusion layer (SGL GROUP, Germany). The electrode was dried in a vacuum oven for 12 h at 100°C to remove the residual NMP solvent. The geometrical area of the carbon air electrode was 1.13 cm^2 and the carbon loading in the air electrode was about 1.0 mg cm^{-2}, unless specified otherwise. The negative electrode consisted of a lithium metal (Honjo Metal Co. Ltd., 100 μm) that was pressed on a copper current collector. The lithium-air cell composed of a lithium electrode, glass microfiber filter paper (Whatman grade GF/D), and a carbon air electrode was assembled with an electrolyte solution into a custom-designed Swagelok-type cell fabricated from Teflon, as schematically depicted in Figure 1. All cells were assembled in an argon-filled glove box where the H_2O and O_2 contents were kept below 1 ppm.

Measurements.— The viscosity of the electrolyte solution was measured using a viscometer (Schott AVS 350). The ionic conductivity of the liquid electrolyte was measured by a Cond 3210 conductivity meter (WTW GmbH, Germany). Linear sweep voltammetry (LSV) was performed to investigate the electrochemical stability of the electrolyte solution on a platinum working electrode with lithium metal counter and reference electrodes at a scanning rate of 1.0 m V s^{-1}. Charge and discharge cycling tests of the lithium-air cells were performed using battery testing equipment (WBCS 3000, Wonatech). For the cycling tests, the cell was placed in a chamber that was filled with high-purity oxygen gas at a pressure slightly higher than 1.0 atm. Charge-discharge curves were recorded galvanostatically at a constant current rate of 100 mA $(g\ carbon)^{-1}$ within a limited capacity of 1,000 mAh g^{-1} in the voltage range of 2.0 to 5.0 V, unless specified

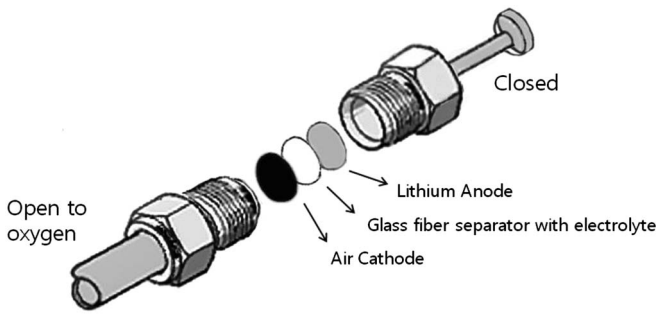

Figure 1. Schematic representation of the Swagelok-type lithium-air cell used in the cycling tests.

*Electrochemical Society Active Member.
zE-mail: dongwonkim@hanyang.ac.kr

Downloaded on 2014-04-18 to IP 166.104.26.40 address. Redistribution subject to ECS terms of use (see ecsdl.org/site/terms_use) unless CC License in place (see abstract).

otherwise. We considered the mass of Ketjen black as the active material loading in the air electrode. The morphologies of the carbon air electrodes were examined using field-emission scanning electron microscopy (FE-SEM, HITACHI S-4800). The XRD patterns of the air electrodes obtained by a powder X-ray diffractometer (XRD, D/MAX RINT 2000) utilizing a CuK_α radiation source after charge and discharge cycling were analyzed to identify the reaction products formed on the electrode. For the XRD measurements, the cells were disassembled in a glove box after cycling. The cathode material was then washed with DEGDEE to remove the residual electrolyte and dried overnight in a vacuum oven. The reaction products formed on the air electrode were analyzed by X-ray photoelectron spectroscopy (XPS) measurements (ESCA 2000, Thermo VG Scientific).

Results and Discussion

The poor cycling stability of lithium-air cells with carbonate-based electrolytes is mainly due to irreversible reactions occurring between oxygen and electrolyte during the discharge process, which produces organic and inorganic carbonate species rather than Li_2O_2.[10,11,21–23] It is well known that ether-based electrolytes such as TEGDME have low sensitivity toward reduced oxygen species compared to carbonate solvents and a low viscosity to facilitate oxygen transport.[24–27] Recently, Xu et al. reported that less Li_2CO_3 and a much higher discharge capacity were observed in Li-O_2 batteries using DEGDBE as the electrolyte solvent compared to using other organic solvents.[28] Furthermore, the formation of dendritic lithium could be remarkably suppressed even at a high current rate.[29] Based on these results, we chose DEGDEE as an alternative ether-based solvent for TEGDME. As presented in Table I, DEGDEE has a glyme structure like TEGDME and DEGDBE. It showed a higher ionic conductivity and lower viscosity to facilitate oxygen and Li^+ ion transport than the TEGDME or DEGDBE-based electrolyte. In addition, since DEGDEE has ethyl groups on the end of the molecule, the electron charge can be more effectively distributed in the molecule compared to molecules containing terminal methyl groups. Thus, it is expected that DEGDEE is more stable against nucleophilic attack by superoxide anion radicals than other glyme family molecules such as TEGDME and dimethoxy ethane.

The linear sweep voltammetry curves of three electrolyte systems in the absence of oxygen are shown in Figure 2. In the anodic scan for the TEGDME-based electrolyte, the anodic current starts to increase around 4.9 V vs. Li/Li^+, which can be attributed to the oxidative decomposition of the electrolyte. It is noticeable that the anodic decomposition with the DEGDEE-based electrolyte was observed at a potential higher than 5.1 V vs. Li/Li^+, which is higher than those of other two electrolytes. From these results, it is expected that the DEGDEE-based electrolyte exhibits more stable electrochemical behavior than the TEGDME or DEGDBE-based electrolyte at high voltages. In the cathodic scan shown in Figure 2b, large reductive currents are observed around 0 V vs. Li/Li^+ for all the electrolyte systems, which correspond to the reductive deposition of lithium onto the electrode (i.e., $Li^+ + e \rightarrow Li$). The absence of significant reduction peaks prior to the lithium plating indicates that the electrolyte systems are reductively stable up to 0 V vs. Li/Li^+. These results indicate that DEGDEE is a promising solvent which is electrochemically stable enough for lithium-air cells.

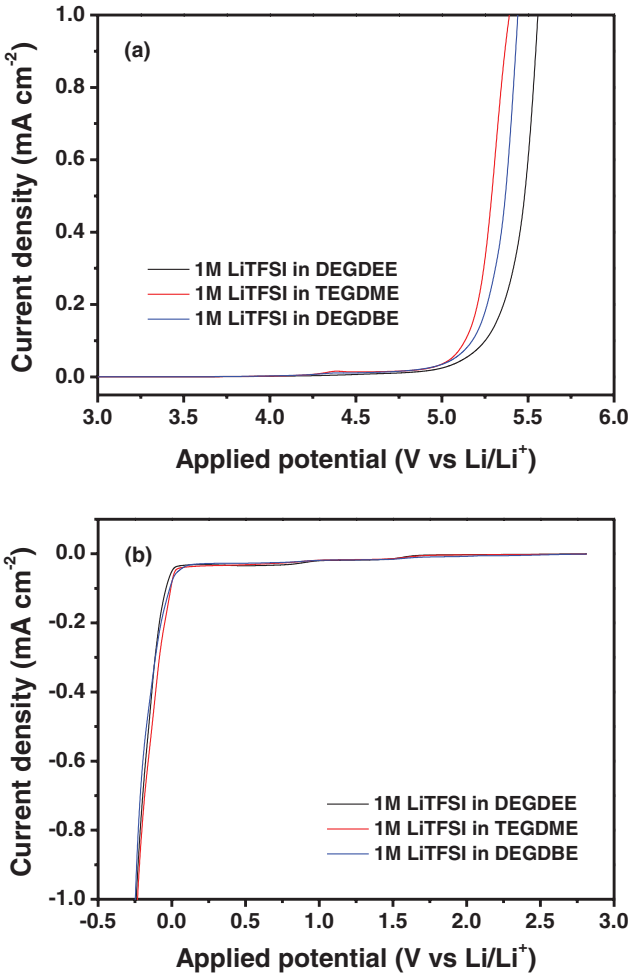

Figure 2. Linear sweep voltammograms of 1 M LiTFSI in DEGDEE, TEGDME and DEGDBE electrolytes without oxygen flow: (a) anodic scan and (b) cathodic scan (scan rate: 1 mV s^{-1}).

The full discharge and charge behaviors of the lithium-air cells assembled with the different electrolyte solutions were investigated at constant current densities of 0.1 mA cm^{-2} and 100 mA g^{-1}. Figure 3 shows the initial three cycles of the cells assembled utilizing the ether-based electrolytes, which were cycled within a cutoff voltage of 2.0–4.5 V. Clearly, the type of the electrolyte solution affected the cycling characteristics of the cell. For the first cycle, the TEGDME-based cell delivered a higher discharge capacity (7,750 mAh g^{-1}, specific capacity is defined per gram of Ketjen Black carbon) than the other two cells, although its discharge capacity drastically decreased in subsequent cycles. Note that the cell with the DEGDEE electrolyte (Figure 3a) delivered relatively stable capacities in subsequent full discharge and charge cycles. In terms of the coulombic efficiency, the DEGDEE-based cell demonstrated noticeably greater columbic

Table I. Molecular structures and physical properties of the different organic solvents, and ionic conductivities of 1.0 M LiTFSI electrolyte in the organic solvents at 25°C (black: carbon atom, red: oxygen atom).

	Molecular structure	Boiling point (°C)	Viscosity (cP)	Conductivity (mS cm^{-1})
DEGDEE	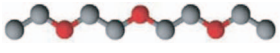	186	1.4	4.7
TEGDME	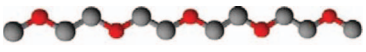	275	4.1	2.8
DEGDBE	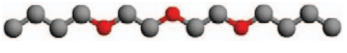	255	2.2	1.4

Downloaded on 2014-04-18 to IP 166.104.26.40 address. Redistribution subject to ECS terms of use (see ecsdl.org/site/terms_use) unless CC License in place (see abstract).

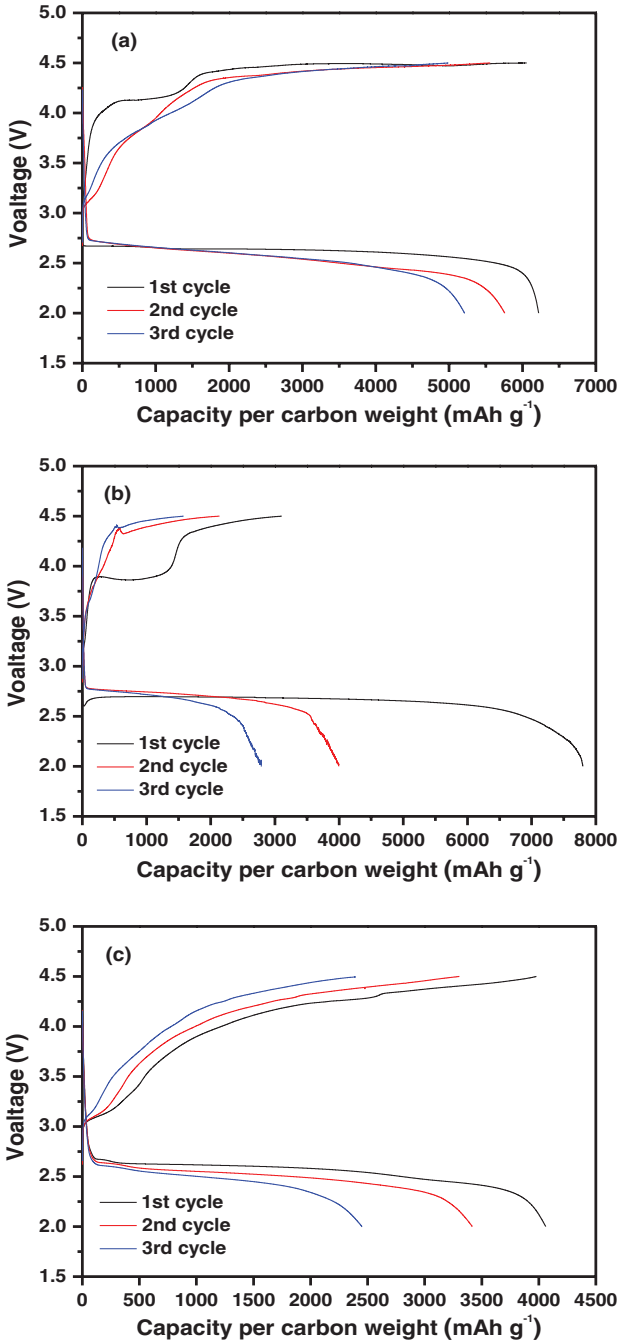

Figure 3. Initial discharge and charge cycles for lithium-air cells assembled with different electrolyte solutions, which are obtained between 2.0 and 4.5 V at a constant current density of 0.1 mA cm^{-2} (100 mA g^{-1}): (a) DEGDEE-based, (b) TEGDME-based, and (c) DEGDBE-based cells. The discharge and charge capacities are normalized by the mass of the Ketjen black powder.

efficiency than the TEGDME-based cell throughout all cycles. This result supports the notion that the reversibility for the oxygen reduction reaction and oxygen evolution reaction ($2Li + O_2 \leftrightarrow Li_2O_2$) in the lithium-air cell with DEGDEE is much higher than in the cell with TEGDME. The DEGDBE-based cell showed a low initial discharge capacity (4,061 mAh g^{-1}) and high overpotentials as a result of a combined effect of the lower ionic conductivity as well as the higher viscosity. Overall, the DEGDEE-based lithium-air cell exhibited the best cycling characteristics with respect to discharge capacity and cycling stability.

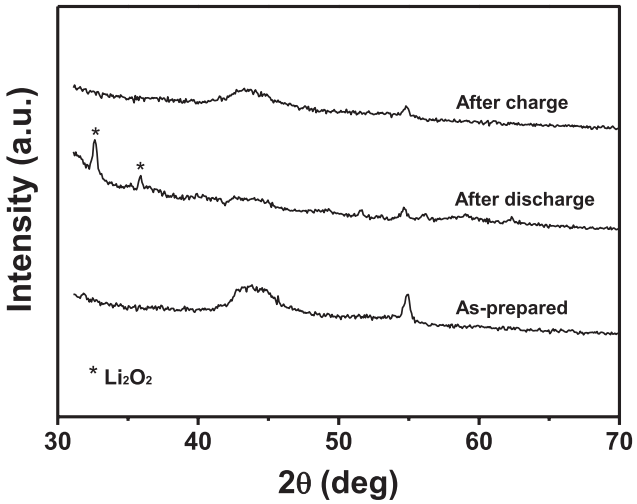

Figure 4. XRD diffraction patterns of a porous carbon electrode analyzed with a cell in its pristine state, after complete discharge, and after complete recharge.

In order to further validate the reversible electrochemical process taking place at the air-cathode in the DEGDEE-based cell, the XRD diffraction patterns of a carbon electrode were analyzed for a cell in its pristine state, after complete discharge, and after complete recharge. Figure 4 shows the powder XRD patterns of the carbon electrode as a function of the state of cycling. From the XRD patterns obtained after full discharge, the characteristics peaks for crystalline Li_2O_2 are clearly observed, as reported earlier.[19,30–32] This result suggests that the DEGDEE electrolyte can lead to the formation of the desired Li_2O_2 with a crystalline structure and DEGDEE is relatively stable to superoxide radical anions which are the single-electron reduction species of oxygen formed during discharge.[33] The absence of Li_2O_2 characteristics peaks in the XRD pattern after recharging shows that all of the discharge products can be fully decomposed, which confirms the reversible formation and decomposition of Li_2O_2 during cycling. The reversibility of the electrochemical process in the DEGDEE-based cell was further confirmed by SEM analyzes carried out on the carbon electrode. A SEM image of the discharged carbon electrode in Figure 5b exhibited uniform coating of reaction products onto the carbon particles, which are believed to be associated with the formation of Li_2O_2.[19,32] The particles in the charged electrode in Figure 5c were very similar to those of a pristine electrode, which is well consistent with XRD results showing a complete decomposition of Li_2O_2 particles deposited on the carbon electrode during the discharge process.

To identify the reaction products formed on the air electrode during discharge process, XPS analysis was performed. Figure 6a and 6b show the O 1s XPS spectra of the air electrodes discharged in DEGDEE and TEGDME, respectively. The main peaks from Li_2O_2 and TFSI anion are observed at 531.0 and 532.7 eV, respectively, which are well consistent with reported binding energies.[34–36] It should be noted that the peak intensity corresponding to Li_2O_2 is much stronger in DEGDEE than TEGDME, indicating that a larger amount of Li_2O_2 is formed on the air electrode cycled in DEGDEE. However, the peak appeared at 532.1 eV, which corresponds to Li_2CO_3,[37] shows the opposite trend. During the discharge process, the superoxide anion radials may attack the alkylene group adjacent to the ether bond of solvent, cause its irreversible decomposition into CO_2 or carbonate groups that in turn form Li_2CO_3 by reacting with Li_2O_2 formed on the air electrode, as previously reported.[11,28] Thus, the XPS results demonstrate that DEGDEE is relatively stable to superoxide anion radicals, resulting in highly reversible oxygen reduction and evolution reaction in the lithium-air cell, as illustrated in Figure 3.

Downloaded on 2014-04-18 to IP 166.104.26.40 address. Redistribution subject to ECS terms of use (see ecsdl.org/site/terms_use) unless CC License in place (see abstract).

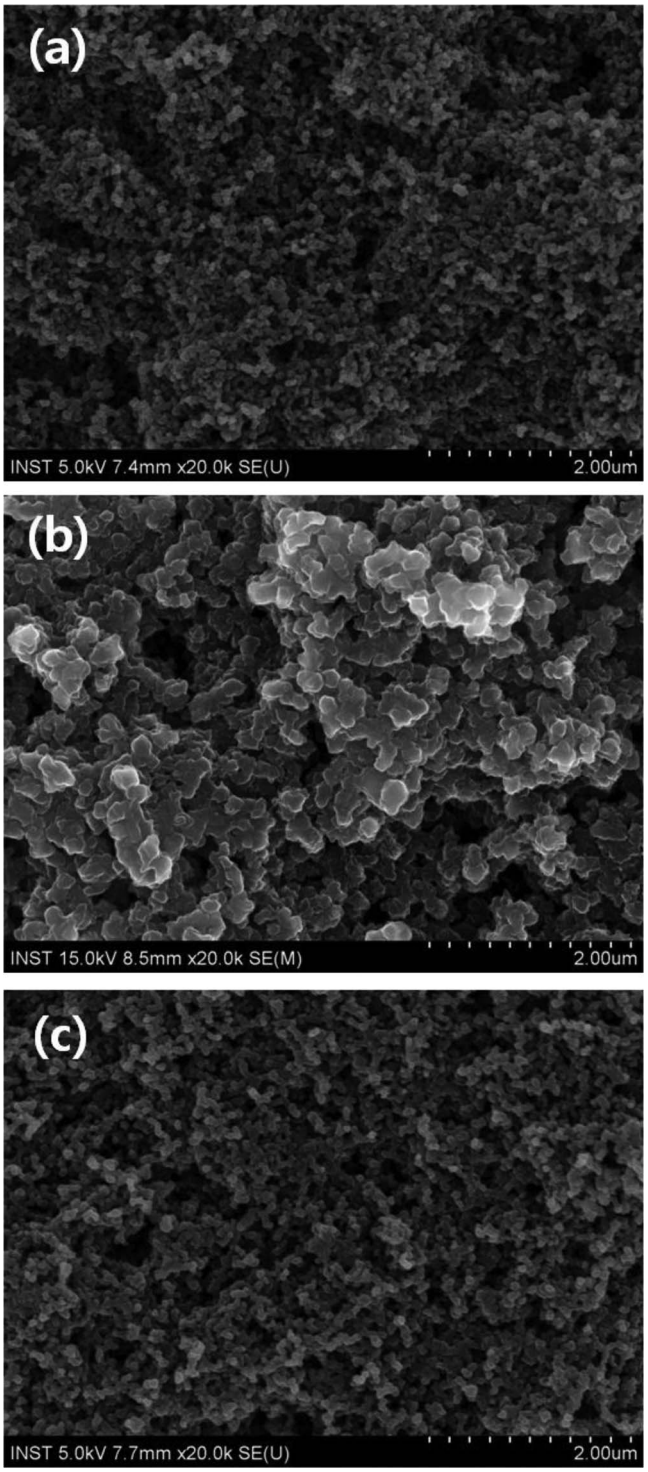

Figure 5. SEM images of the air electrodes in the DEGDEE-based cell (a) before discharge (pristine), (b) in the discharge state at 2.0 V and (c) in the charged state at 4.5 V.

The rate capability of the lithium-air cell assembled with the DEGDEE electrolyte was evaluated. After the cell assembly, the cells were fully discharged to a cutoff voltage of 2.0 V at different current densities ranging from 0.1 to 0.4 mA cm^{-2}, as shown in the voltage profiles presented in Figure 7. As expected, the current density affects the specific capacity of the lithium-air cell. Both the discharge voltage plateau and discharge capacity decreased with increasing current density. Increasing the current density from 0.1 to 0.4 mA cm^{-2}

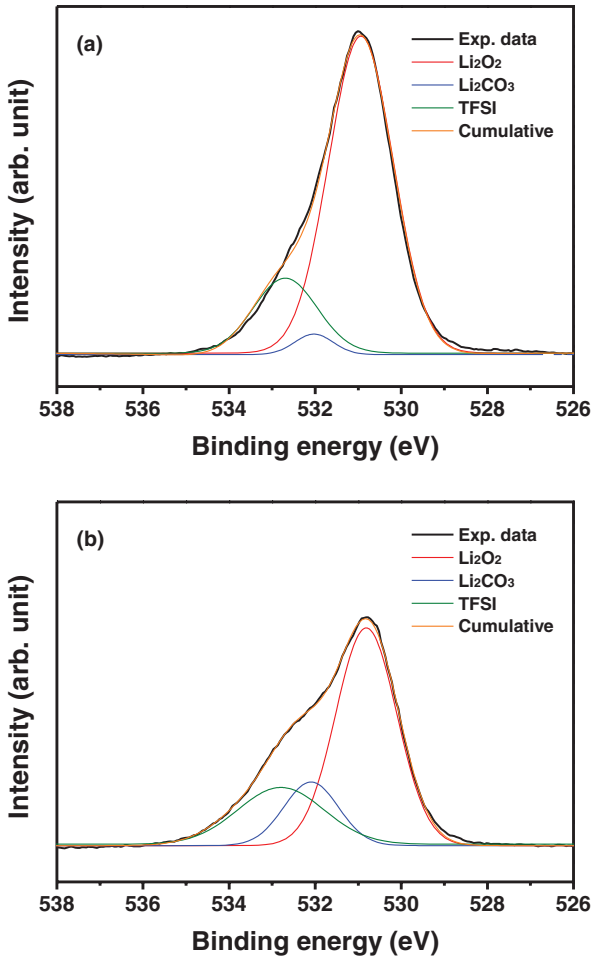

Figure 6. XPS spectra (O 1s) of the air electrodes discharged in (a) DEGDEE and (b) TEGDME.

considerably decreased the specific discharge capacity from 6,219 to 1,251 mAh g^{-1}. This result is due to the slow kinetics of the oxygen reduction reaction at the air cathode without a catalyst, and has to be improved. The use of an oxygen catalyst may facilitate the oxygen reduction reaction and therefore reduce polarization, which requires further studies. Although the high rate performance of the cell with DEGDEE is far from being satisfactory, it should be noted that the

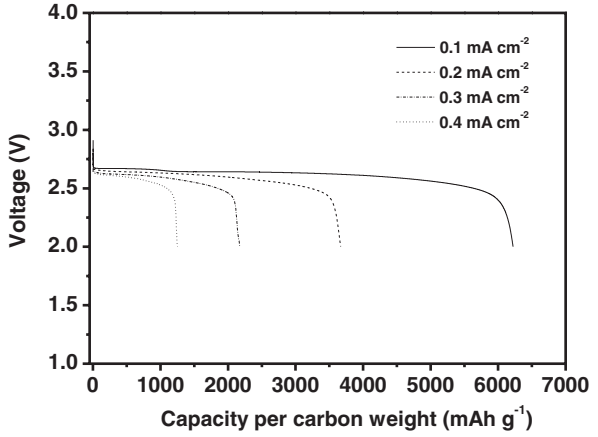

Figure 7. Initial discharge curves of the lithium-air cell with 1.0 M LiTFSI-DEGDEE electrolyte under different current densities where the carbon loading in the air cathode was 1.0 mg cm^{-2}.

Downloaded on 2014-04-18 to IP 166.104.26.40 address. Redistribution subject to ECS terms of use (see ecsdl.org/site/terms_use) unless CC License in place (see abstract).

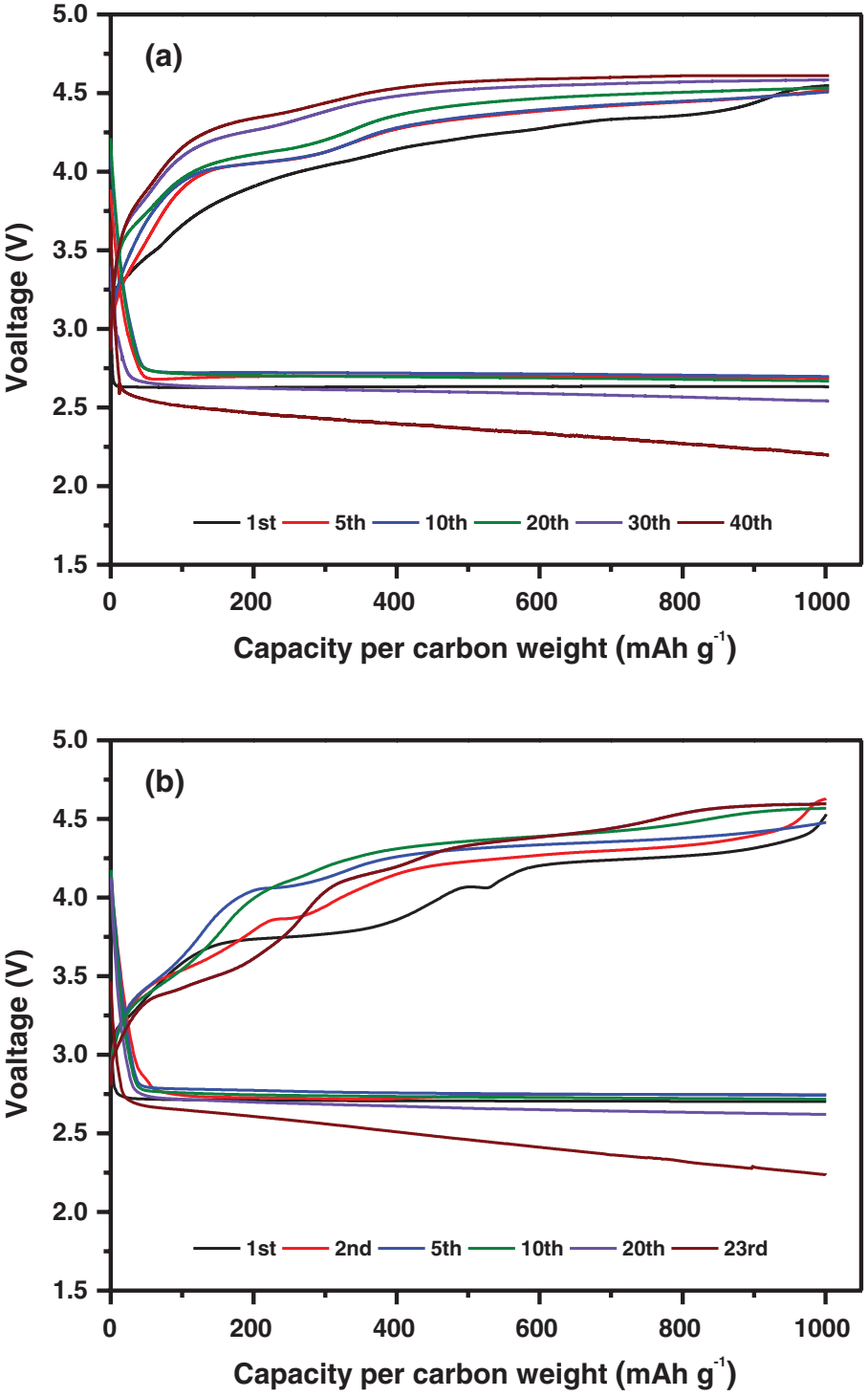

Figure 8. Discharge and charge curves of the lithium-air cells assembled with different electrolyte solutions at a constant current density of 0.1 mA cm^{-2} (100 mA g^{-1}) where the carbon loading in the air cathode was 1.0 mg cm^{-2}: (a) DEGDEE-based electrolyte and (b) TEGDME-based electrolyte.

specific capacity at high current densities is higher than those obtained in lithium-air cells with other organic solvents.[31,38]

The buildup of insoluble discharge products in a fully discharged cell may inhibit the transport of lithium ions, oxygen, and electrons to the electrochemical interface, which leads to permanent choking of a porous carbon electrode after a few cycles.[39,40] In order to avoid accumulation of the insulating discharge products, the capacity utilization was limited to 1,000 mAh g^{-1}. Figure 8a shows the discharge and charge curves of the lithium-air cell assembled with the DEEDEE-based electrolyte obtained by controlling the discharge depth to 1,000 mAh g^{-1} at a constant current density of 0.1 mA cm^{-2} (100 mA g^{-1}). Reversible charge and discharge cycling was observed during repeated cycles up to 40 cycles. However, the polarization for the charge and discharge cycles increased with cycle number. This result may be attributed to the inability to oxidize the non-conducting discharge product Li_2O_2 in the pores of the carbon cathode due to the increased cell resistance and associated overpotential of the electrode during cycling. In case of the cell with TEGDME-based electrolyte, the gap between the charge and discharge profiles becomes more significant over cycling compared with that of the DEGDEE-based cell, as shown in Figure 8b. The poor cycling stability of TEGDME-based cell can be ascribed to the accumulation of the irreversible products generated from the electrolyte decomposition, as explained earlier in Figure 6.

Downloaded on 2014-04-18 to IP 166.104.26.40 address. Redistribution subject to ECS terms of use (see ecsdl.org/site/terms_use) unless CC License in place (see abstract).

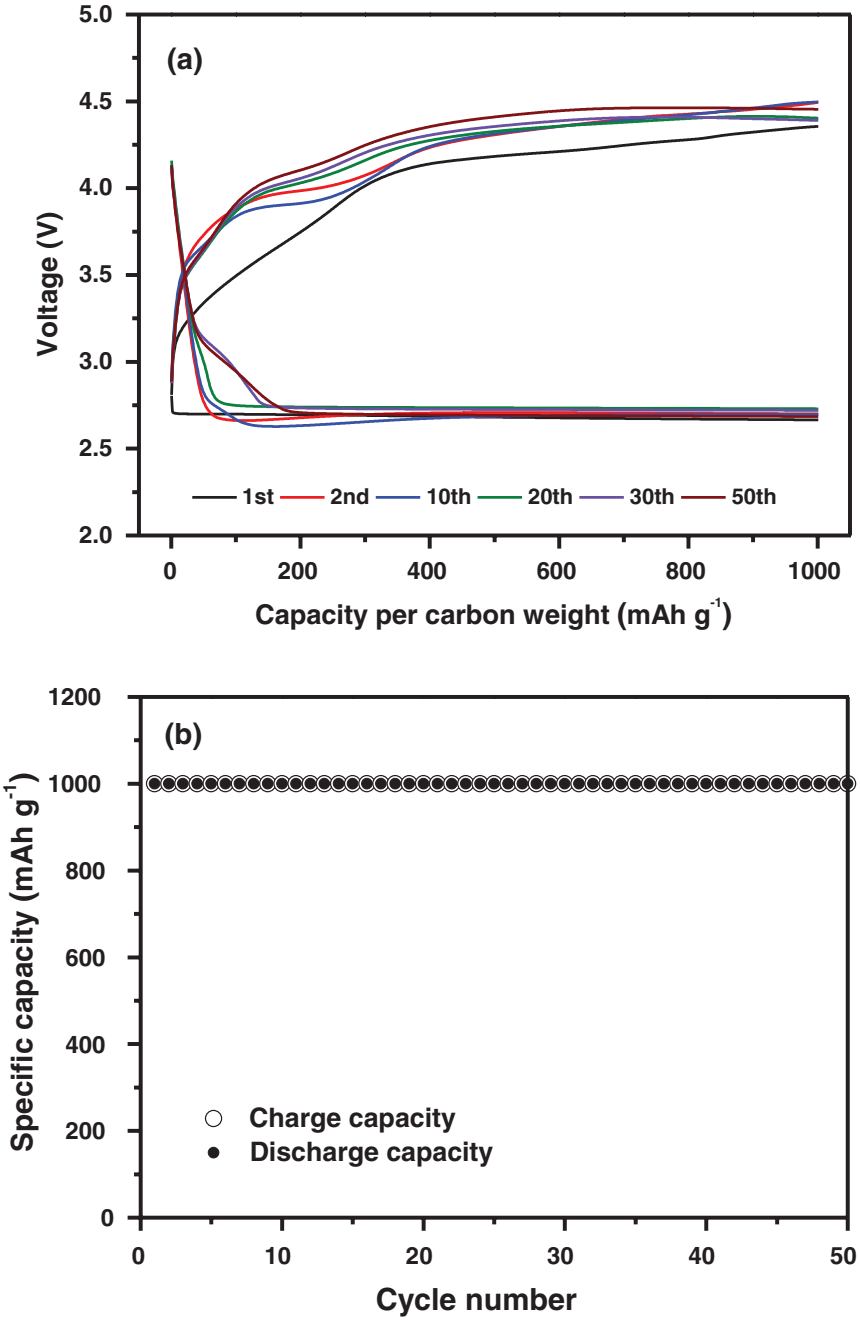

Figure 9. (a) Discharge and charge curves of the lithium-air cell with 1.0 M LiTFSI- DEGDEE electrolyte at a constant current density of 0.05 mA cm^{-2} (100 mA g^{-1}), and (b) discharge and charge capacities as a function of the cycle number for the same cell. The carbon loading in the air cathode was 0.5 mg cm^{-2}.

In order to improve the cycling stability of the lithium-air cell, the carbon loading was reduced to from 1.0 to 0.5 mg cm^{-2}. The cell was cycled at a constant current density of 0.05 mA cm^{-2} (100 mA g^{-1}) within a limited capacity of 1,000 mAh g^{-1}. Figure 9a shows the charge and discharge profiles of the lithium-air cell assembled with a carbon electrode at a carbon loading of 0.5 mg cm^{-2} as a function of the cycle number. Interestingly, there were no significant changes of the voltage profiles over 50 cycles except for the first cycle, indicating good charge-discharge cycling stability with a coulombic efficiency of 100%, as depicted in Figure 9b. As the cell discharges, passivation of the carbon electrode occurs via the formation of the insoluble and insulating Li_2O_2 product. When the carbon loading in the electrode is decreased, the amount of discharge products deposited on the surface of the carbon electrode can be reduced, which may suppress permanent choking of the carbon electrode and also reduce electrode polarization. Also, the transport of oxygen into the interior of the carbon electrode will be facilitated more when using a thinner electrode. Accordingly, the data in Figure 8 and 9 imply that the capacity retention of the lithium-air cell with the DEGDEE-based electrolyte can be improved by employing a proper engineering design of the air cathode considering its thickness, porosity and the volume fraction of carbon black. More studies are currently in progress in order to achieve good cycling stability while maintaining a relatively high amount of carbon loading in the air electrode.

Conclusions

We proposed and demonstrated a novel DEGDEE-based electrolyte for use in lithium-air cells. The electrolyte solution of 1 M LiTFSI in DEGDEE showed a higher ionic conductivity, lower viscosity and higher oxidative stability than the TEGDME or DEGDBE-based electrolyte. The formation of Li_2O_2 and its reversibility were confirmed by full discharge/charge cycles, XRD, SEM and XPS analyzes, which makes DEGDEE an appropriate solvent for lithium-air

Downloaded on 2014-04-18 to IP 166.104.26.40 address. Redistribution subject to ECS terms of use (see ecsdl.org/site/terms_use) unless CC License in place (see abstract).

cells. The lithium-air cell assembled with the DEGDEE-based electrolyte and carbon electrode exhibited stable cycling behavior when constraining the carbon loading to 0.5 mg cm^{-2} and limiting the depth of discharge to 1,000 mAh g^{-1}. We believe that our results will open up new possibilities to promote the development of rechargeable lithium-air batteries with good cyclability.

Acknowledgments

This work was supported by the Energy Efficiency & Resources (No. 20112010100110) and Human Resources Development Program (No. 20124010203290) of the Korea Institute of Energy Technology Evaluation and Planning (KETEP) grant funded by the Korea government Ministry of Trade, Industry and Energy.

References

1. K. M. Abraham and Z. Jiang, *J. Electrochem. Soc.*, **143**, 1 (1996).
2. J. P. Zheng, R. Y. Liang, M. Hendrickson, and E. J. Plichta, *J. Electrochem. Soc.*, **155**, A432 (2008).
3. J. Christensen, P. Albertus, R. S. Sanchez-Carrera, T. Lohmann, B. Kozinsky, R. Liedtke, J. Ahmed, and A. Kojica, *J. Electrochem. Soc.*, **159**, R1 (2012).
4. G. Girishkumar, B. McCloskey, A. C. Luntz, S. Swanson, and W. J. Wilcke, *J. Phys. Chem. Lett.*, **1**, 2193 (2010).
5. P. G. Bruce, S. A. Freunberger, L. J. Hardwick, and J.-M. Tarascon, *Nature Mater.*, **11**, 19 (2012).
6. F. Cheng and J. Chen, *Chem. Soc. Rev.*, **41**, 2172 (2012).
7. Y. Shao, F. Ding, J. Xiao, J. Zhang, W. Xu, S. Park, J.-G. Zhang, Y. Wang, and J. Liu, *Adv. Funct. Mater.*, **23**, 987 (2013).
8. V. S. Bryantsev, J. Uddin, V. Giordani, W. Walker, D. Addison, and G. V. Chase, *J. Electrochem. Soc.*, **160**, A160 (2013).
9. C. O. Laoire, S. Mukerjee, E. J. Plichta, M. A. Hendrickson, and K. M. Abraham, *J. Electrochem. Soc.*, **158**, A302 (2011).
10. B. D. McCloskey, D. S. Bethune, R. M. Shelby, G. Girishkumar, and A. C. Luntz, *J. Phys. Chem. Lett.*, **2**, 1161 (2011).
11. S. A. Freunberger, Y. Chen, Z. Peng, J. M. Griffin, L. J. Hardwick, F. Barde, P. Novak, and P. G. Bruce, *J. Am. Chem. Soc.*, **133**, 8040 (2011).
12. W. Xu, V. V. Viswanathan, D. Wang, S. A. Towne, J. Xiao, Z. Nie, D. Hu, and J.-G. Zhang, *J. Power Sources*, **196**, 3894 (2011).
13. G. M. Veith, N. J. Dudney, J. Howe, and J. Nanda, *J. Phys. Chem. C*, **115**, 14325 (2011).
14. S. A. Freunberger, Y. Chen, N. E. Drewett, L. J. Hardwick, F. Barde, and P. G. Bruce, *Angew. Chem., Int. Ed.*, **50**, 8609 (2011).
15. H. Wang and K. Xie, *Electrochim. Acta*, **64**, 29 (2012).
16. D. Sharon, M. Afri, M. Noked, A. Garsuch, A. A. Frimer, and D. Aurbach, *J. Phys. Chem. Lett.*, **4**, 3115 (2013).
17. J. R. Harding, Y.-C. Lu, Y. Tsukada, and Y. Shao-Horn, *Phys. Chem. Chem. Phys.*, **14**, 10540 (2012).
18. G. M. Veith, J. Nanda, L. H. Delmau, and N. J. Dudney, *J. Phys. Chem. Lett.*, **3**, 1242 (2012).
19. H.-G. Jung, J. Hassoun, J.-B. Park, Y.-K. Sun, and B. Scrosati, *Nature Chem.*, **4**, 579 (2012).
20. H.-D. Lim, K.-Y. Park, H. Gwon, J. Hong, H. Kim, and K. Kang, *Chem. Commun.*, **48**, 8374 (2012).
21. V. S. Bryantsev and M. Blanco, *J. Phys. Chem. Lett.*, **2**, 379 (2011).
22. J. Xiao, J. Hu, and Z. J. Nie, *J. Power Sources*, **196**, 5674 (2011).
23. J. Hassoun, F. Croce, and B. Scrosati, *Angew. Chem. Int. Ed.*, **50**, 2999 (2011).
24. D. Aurbach, M. Daroux, P. Faguy, and E. Yeager, *J. Electroanal. Chem. Interfacial Electrochem.*, **297**, 225 (1991).
25. V. S. Bryantsev, V. Giordani, W. Walker, M. Blanco, S. Zecevic, K. Sasaki, J. Uddin, D. Addison, and G. V. Chase, *J. Phys. Chem. A*, **115**, 12399 (2011).
26. J. Read, *J. Electrochem. Soc.*, **153**, A96 (2006).
27. K. U. Schwenke, S. Meini, X. Wu, H. A. Gasteiger, and M. Piana, *Phys. Chem. Chem. Phys.*, **15**, 11830 (2013).
28. W. Xu, J. Hu, M. H. Engelhard, S. A. Towne, J. S. Hardy, J. Xiao, J. Feng, M. Y. Hu, J. Zhang, F. Ding, M. E. Gross, and J.-G. Zhang, *J. Power Sources*, **215**, 240 (2012).
29. K. Xu, *Chem Rev.*, **104**, 4303 (2004).
30. H. G. Jung, H. S. Kim, J. B. Park, I. H. Oh, J. Hassoun, C. S. Yoon, B. Scrosati, and Y. K. Sun, *Nano Lett.*, **12**, 4333 (2012).
31. D. Xu, Z. Wang, J. Xu, L. Zhang, and X. Zhang, *Chem. Commun.*, **48**, 6948 (2012).
32. D. Sharon, V. Etacheri, A. Garsuch, M. Afri, A. A. Frimer, and D. Aurbach, *J. Phys. Chem. Lett.*, **4**, 127 (2013).
33. C. O. Laoire, S. Mukerjee, K. M. Abraham, E. J. Plichta, and M. A. Hendrickson, *J. Phys. Chem. C*, **114**, 9178 (2010).
34. G. M. Veith, J. Nanda, L. H. Delmau, and N. J. Dudney, *J. Phys. Chem. Lett.*, **3**, 1242 (2012).
35. B. G. Kim, J. N. Lee, D. J. Lee, J. K. Park, and J. W. Choi, *ChemSusChem*, **6**, 443 (2013).
36. S. Men, K. R. J. Lovelock, and P. Licence, *Phys. Chem. Chem. Phys.*, **13**, 15244 (2011).
37. Y.-C. Lu, A. N. Mansour, N. Yabuuchi, and Y. Shao-Horn, *Chem. Mat.*, **21**, 4408 (2009).
38. J. Read, *J. Electrochem. Soc.*, **149**, A1190 (2002).
39. T. Ogasawara, A. Debart, M. Holzapfel, P. Novak, and P. G. Bruce, *J. Am. Chem. Soc.*, **128**, 1390 (2006).
40. M. J. Trahan, S. Mukerjee, E. J. Plichta, M. A. Hendrickson, and K. M. Abraham, *J. Electrochem. Soc.*, **160**, A259 (2013).

Downloaded on 2014-04-18 to IP 166.104.26.40 address. Redistribution subject to ECS terms of use (see ecsdl.org/site/terms_use) unless CC License in place (see abstract).